

**Targeting CAR-Nrf2 improves cyclophosphamide bioactivation while
reducing doxorubicin-induced cardiotoxicity in triple-negative breast cancer
treatment**

Sydney Stern¹, Dongdong Liang¹, Linhao Li¹, Ritika Kurian¹, Caitlin Lynch², Srilatha Sakamuru², Scott Heyward³, Junran Zhang⁴, Kafayat Ajoke Kareem⁵, Young Wook Chun⁵, Ruili Huang², Menghang Xia², Charles Hong⁵, Fengtian Xue^{1*}, and Hongbing Wang^{1*}

¹Department of Pharmaceutical Sciences, University of Maryland School of Pharmacy, 20 Penn Street, Baltimore, Maryland, USA. ²National Center for Advancing Translational Science (NCATS/NIH), 9800 Medical Center Drive, Rockville, Maryland, USA. ³Bioreclamation In Vitro Technologies, 1450 S Rolling Rd, Halethorpe, Maryland, USA. ⁴Department of Radiation Oncology, The Ohio State University James Comprehensive Cancer Center and College of Medicine, Ohio, USA. ⁵Division of Cardiovascular Medicine, University of Maryland School of Medicine, 670 Baltimore Street, Baltimore, Maryland, USA.

Supplementary List

Supplementary Figures: S1-S10

Supplementary Tables: S1-S3

Supplementary Methods

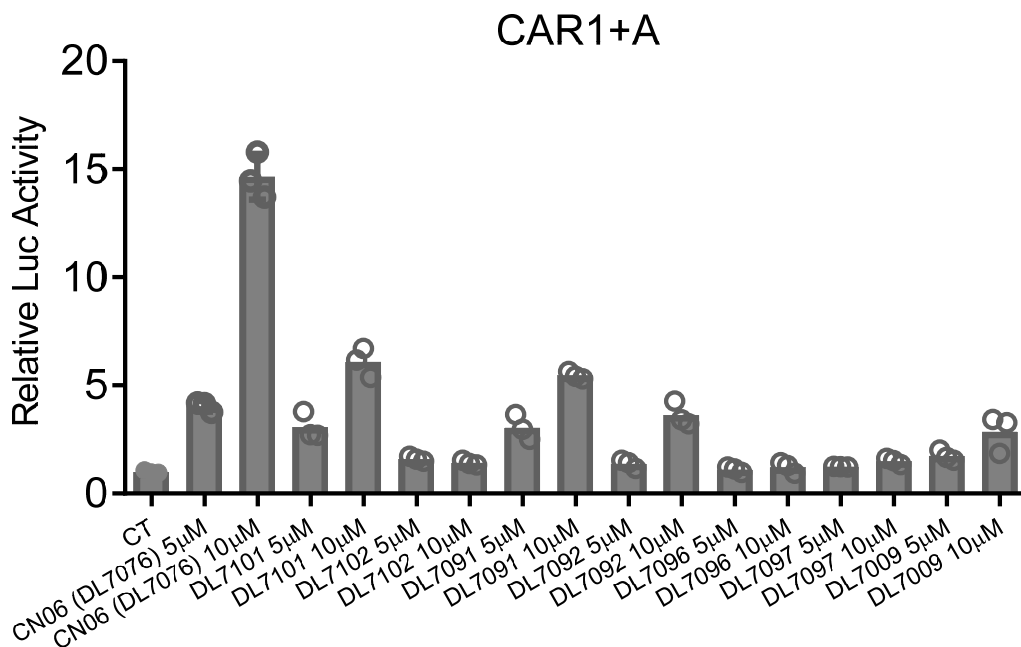


Figure S1. Activation of CAR1+A by chemical analogues of CN06 (DL7076) in HepG2 cells.

HepG2 cells were co-transfected with a CYP2B6-2.2k luciferase reporter plasmid, a PRL-TK vector (Rinella control), and a plasmid expression hCAR1+A, a mutant of hCAR with low basal activity, as detailed in *Material and Methods*. Twenty-four hours after transfection, cells were treated with vehicle control (CT, 0.1% DMSO) or 8 compound analogues of CN06 at 5 µM and 10 µM each for another 24 h. A dual-luciferase assay was utilized to detect the luciferase activities. All values are presented as fold change vs. vehicle control. Results are expressed as mean ± SD (n=3).

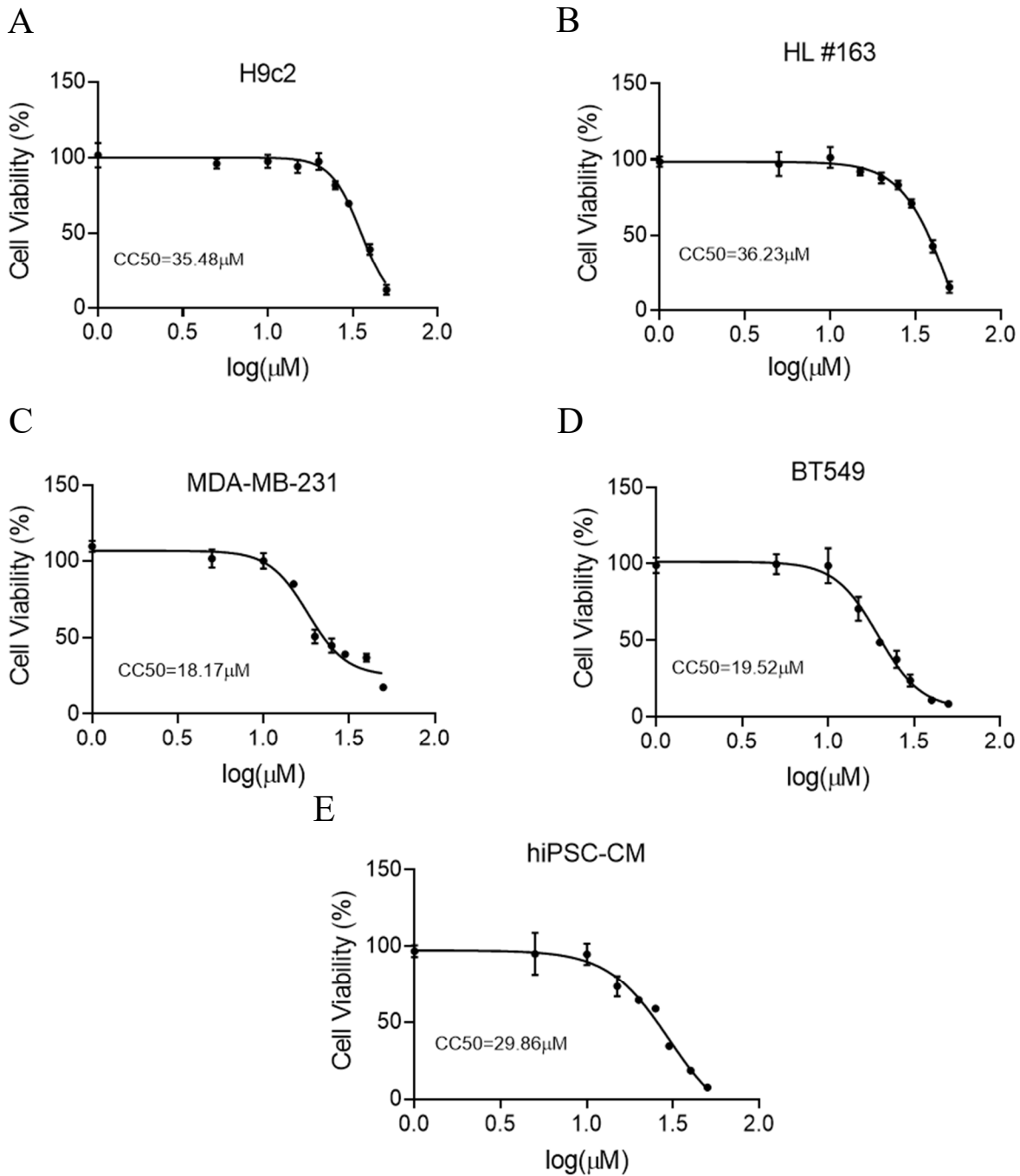


Figure S2. CN06-induced cell death in various types of cultured cells. H9c2 cardiomyocytes (A), human primary hepatocytes (HPH; B), MDA-MB-231 (C), BT549 (D), and hiPSC-derived cardiomyocytes (hiPSC-CMs; E) were cultured in their specific medium and condition as outlined in *Materials and Methods* and treated with CN06 at 0, 1, 5, 10, 15, 20, 25, 30, 40, 50 μM for 24 h. CCK-8 assay was carried out per the manufacturer's instructions. The 50%

cytotoxic concentration (CC50) values were calculated using GraphPad Prism v.7. Triplicate samples were collected at each treatment concentrations (n = 3).

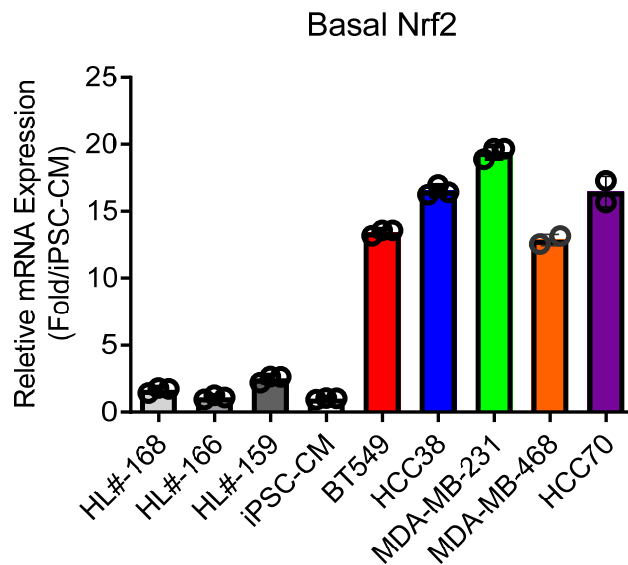


Figure S3. Endogenous expression of Nrf2 in human primary hepatocytes, hiPSC-CMs, and TNBC cell lines. Total RNA was isolated from cultured HPH from three donors (HL#159, #166, and #168), hiPSC-CMs, and five TNBC cell lines (BT549, HCC38, MDA-MB-231, MDA-MB-468, and HCC70), respectively. Relative expression of Nrf2 mRNA was evaluated using RT-PCR. All values are presented as fold changes normalized to the level of hiPSC-CMs, which was designated as 1. Results are expressed as mean \pm SD (n=3).

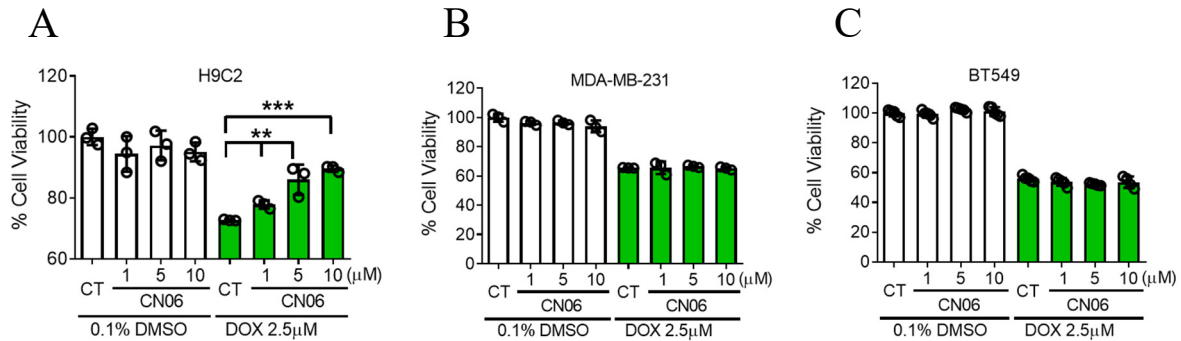


Figure S4. Evaluation of cell viability in H9c2, MDA-MB-231, and BT549 cells treated with CN06 and/or DOX. Relative cell viability was evaluated for ATP generation in H9c2 (A), MDA-MB-231 (B), and BT549 (C) using Cell Titer Glo according to the manufacturer's instructions. Cells were pre-treated for 2 h with CN06 (1, 5, 10 µM) and co-treated with the vehicle control or DOX (2.5 µM) as indicated for 24 h. Relative cell viabilities are presented as percentage changes normalized to the level of the luminescence for the vehicle control, which was designated as 100%. Results are expressed as mean \pm SD (n=3). Data were analyzed using One-Way ANOVA with Bonferroni post hoc. Statistical significance was determined at: **, $P < 0.01$, ***, $P < 0.001$.

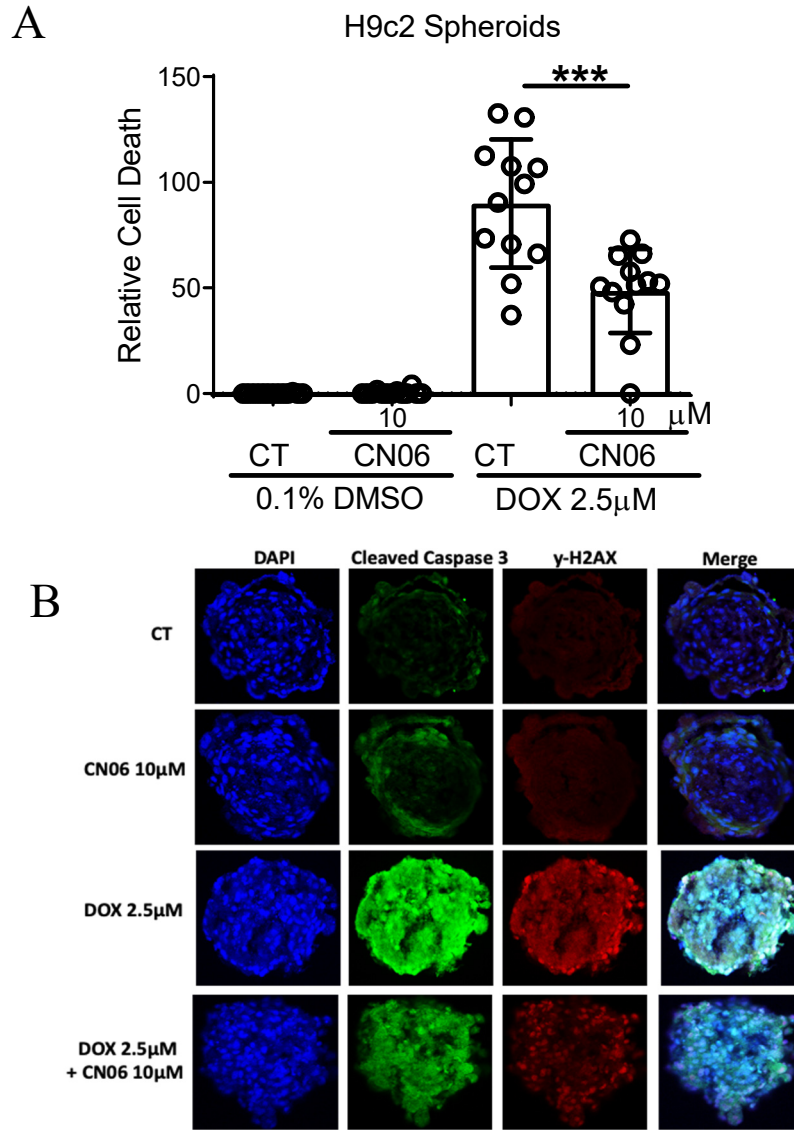


Figure S5. Evaluation of cell viability, DNA damage, and apoptosis in H9c2 spheroids treated with DOX in the presence and absence of CN06. The formation and maintenance of H9c2 spheroids were described in *Supplementary Methods*. Spheroids were then pre-treated with 0.1% DMSO (CT) or CN06 (10 μM) for 2 h followed by co-treatment with DOX (2.5 μM) for 24 h. Cell viability in the spheroids was measured using the NucBlue Live ReadyProbe (R37605, Thermofisher) and NucRed Dead 647 ReadyProbe (R37113, Thermofisher) Reagents following the manufacturer's instructions. Ratio of dead over live cells was quantified using the Celigo

Image Cytometer (Nexcelom) from 12 spheroids/group (A) (Data represents mean \pm SD, 2-tailed Students' t test). In separate experiment, spheroids were immune-stained for cleaved-caspase 3 and γ -H2AX as described in *Supplementary Methods*. Images from each treatment group were demonstrated (B). ***, $P < 0.001$.

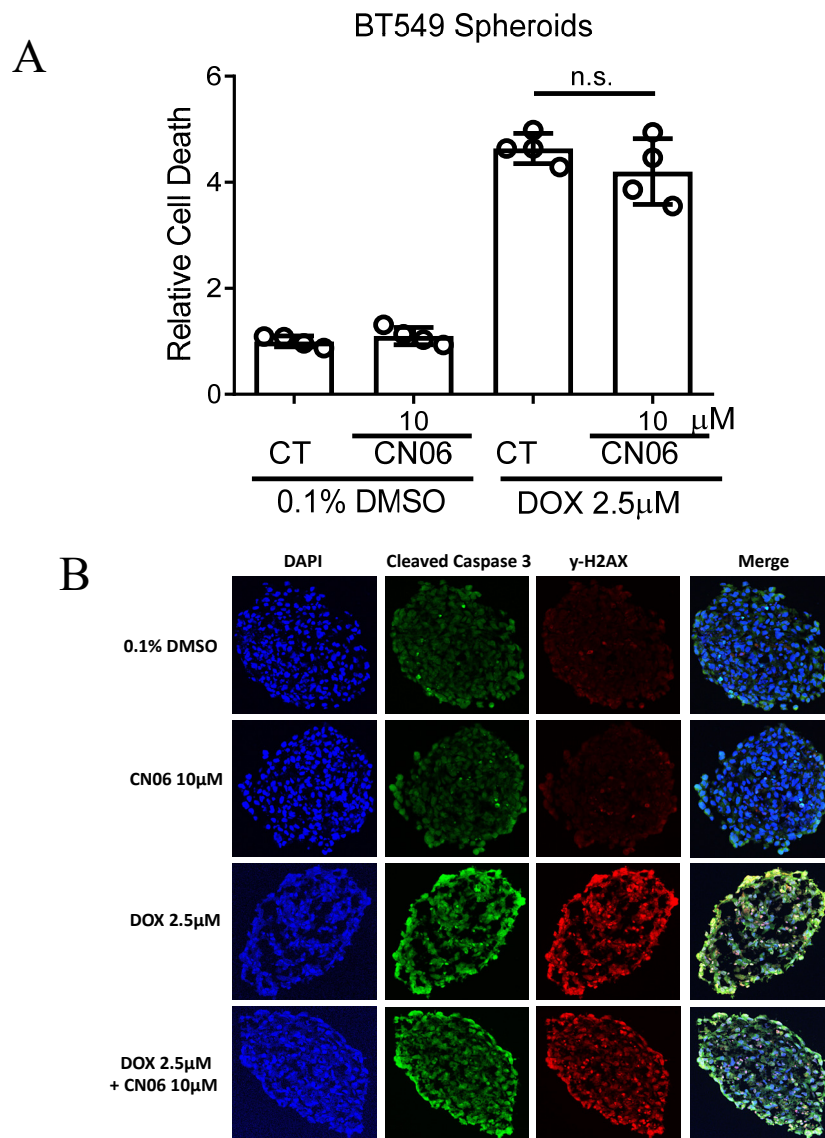


Figure S6. Evaluation of cell viability, DNA damage, and apoptosis in BT549 spheroids treated with DOX in the presence and absence of CN06. BT549 spheroids were pre-treated with 0.1% DMSO (CT) or CN06 (10 μ M) for 2 h followed by co-treatment with DOX (2.5 μ M)

for 24 h. Cell viability in the spheroids was measured using the NucBlue Live ReadyProbe (R37605, Thermofisher) and NucRed Dead 647 ReadyProbe (R37113, Thermofisher) Reagents following the manufacturer's instructions. Ratio of dead over live cells was quantified using the Celigo Image Cytometer (Nexcelom) from 4 spheroids/group (A) (Data represents mean \pm SD, 2-tailed Students' t test). In separate experiment, spheroids were immune-stained for cleaved-caspase 3 and γ -H2AX as described in *Supplementary Methods*. Images from each treatment group were demonstrated (B). n.s, no significance.

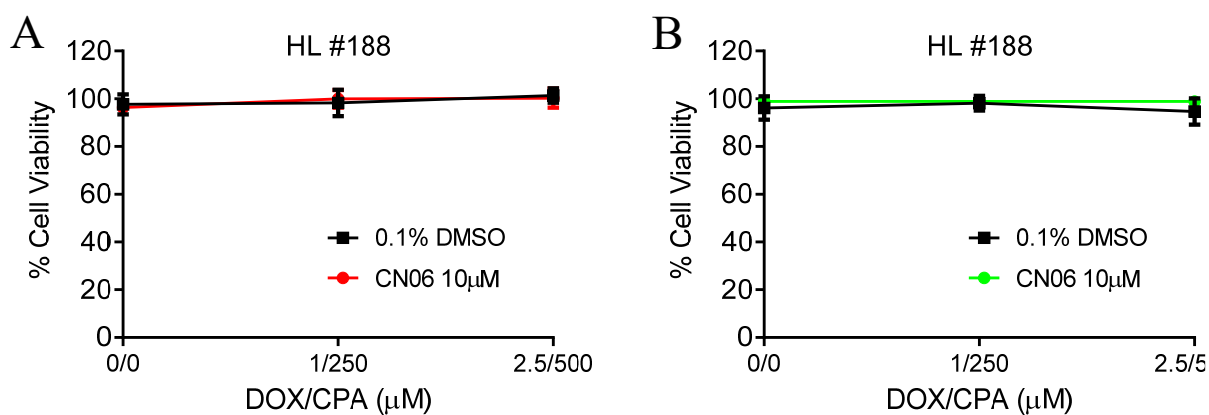


Figure S7. Evaluation of the effect of DOX/CPA combinations on the viability of human primary hepatocytes (HPH) with and without CN06. HPH prepared from liver donor #188 were cultured as detailed in *Materials and Methods*. Cultured hepatocytes were pre-treated for 24 h with 0.1% DMSO or CN06 (10 μM) then co-treated with the combination of DOX/CPA at 0/0, 1/250/, and 2.5/500 μM for another 24 h. Percent cell viability was evaluated by using CCK8 (A) and Cell Titer Glo (B) assays, respectively, as outlined elsewhere. Values (% cell viability) presented are normalized to the vehicle control, which was designated as 100%. Results are expressed as mean \pm SD (n=3).

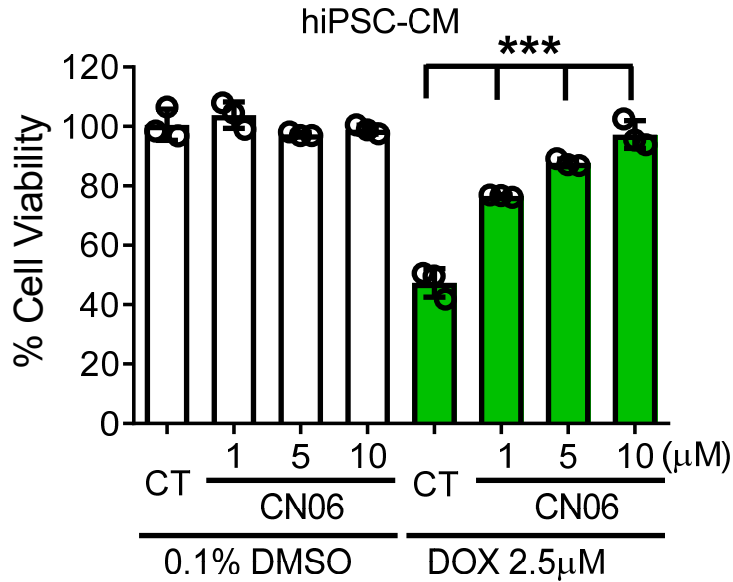


Figure S8. Evaluation of cell viability in hiPSC-CM treated with CN06 and/or DOX.

Human iPSC-CM were differentiated and cultured as outlined in the Materials and Methods. Differentiated hiPSC-CMs were pretreated with 0.1% DMSO (CT) or CN06 (1, 5, and 10 μM) for 2 h, followed by a cotreatment with/without DOX (2.5 μM) for another 24 h. Cell viability was determined using Cell Titer Glo luminescent assay according to the manufacturer's instructions. Percentage of cell viabilities are presented as normalized to the luminescence of the vehicle control, which was designated as 100%. Results are expressed as mean \pm SD (n=3). Data were analyzed using One-Way ANOVA with Bonferroni post hoc. Statistical significance was determined at: ***, $P < 0.001$.

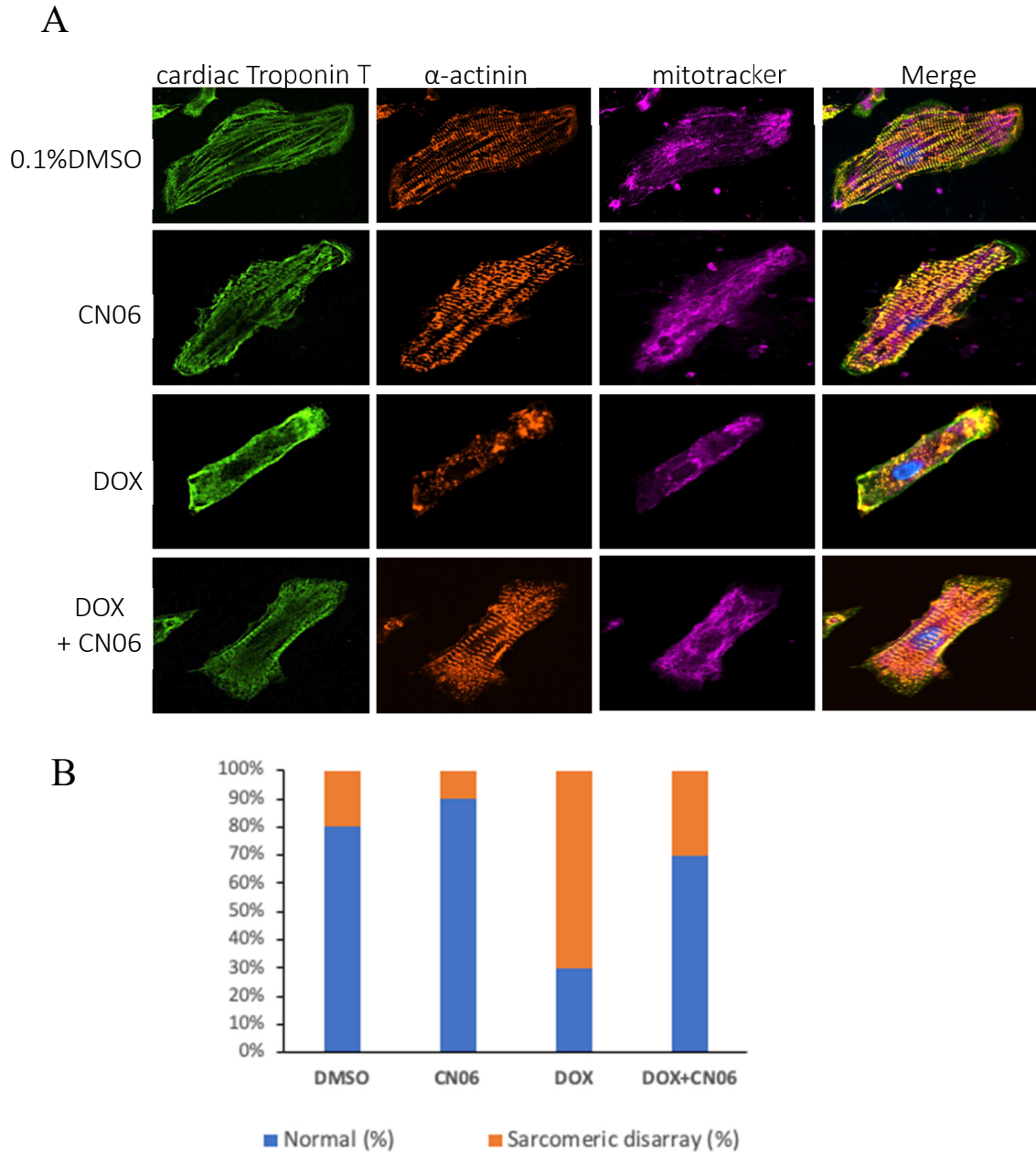


Figure S9. Evaluation of hiPSC-CM cytoskeletal structure following DOX treatment in the presence and absence of CN06. Differentiated hiPSC-CMs were pretreated with 0.1% DMSO or CN06 (10 μ M) for 24 h followed by a cotreatment with DOX (1 μ M) for another 24 h. Subsequently, hiPSC-CMs were treated for 30 mins with mitotracker at RT, fixed with 4% paraformaldehyde, and permeabilized using 0.1% Triton-X. Immuno-staining of cardiac Troponin

T and alpha actinin was performed as outlined in *Supplementary Methods*. Fluorescence microscopy was used to visualize protein expression and distribution (A). Normal sarcomere structure was observed as extensive bundles of myosin-containing filaments while sarcomeric disarray was defined as attenuated and disrupted sarcomeres. Ten cells per condition were determined as normal vs sarcomeric disarray to give an overall percentage of sarcomeric disarray (B).

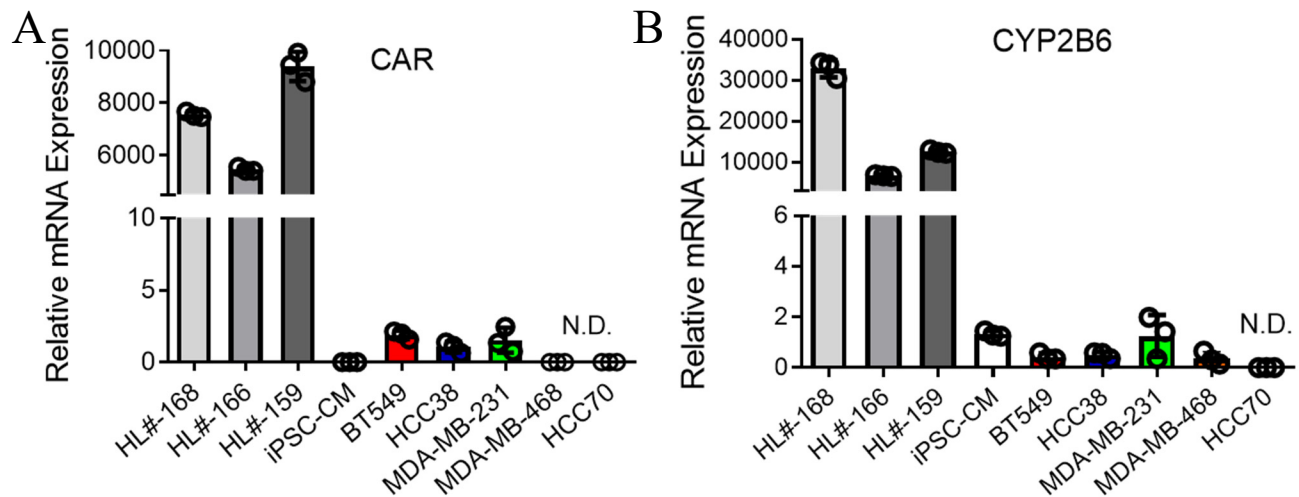
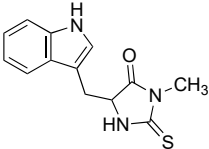
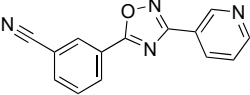
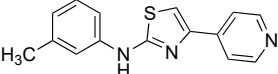
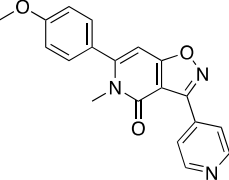
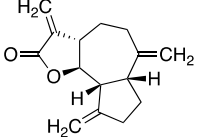
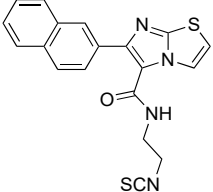
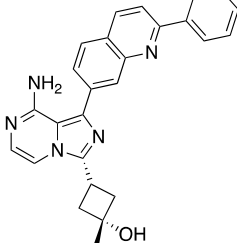
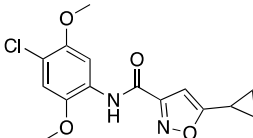
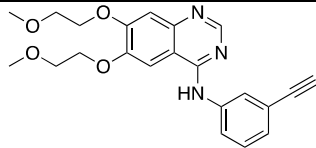
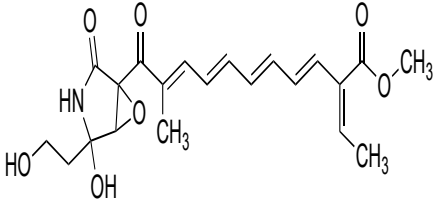
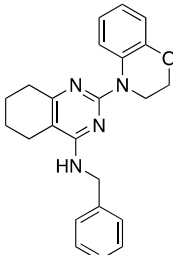
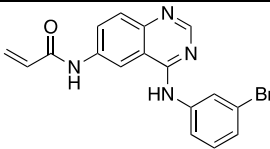
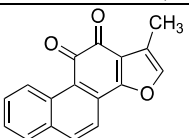
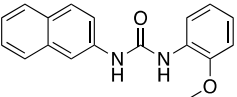
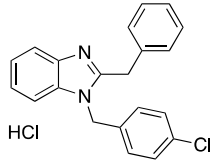
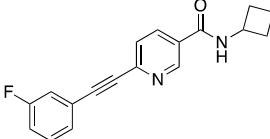
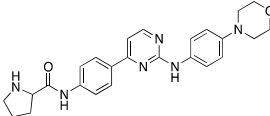


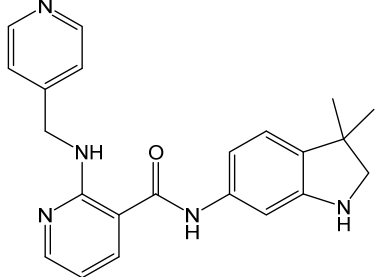
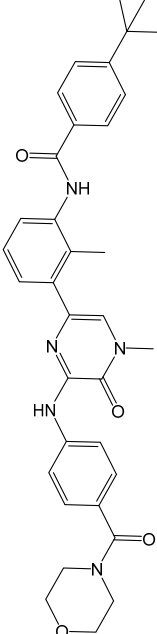
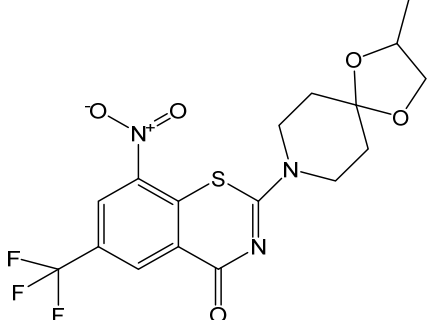
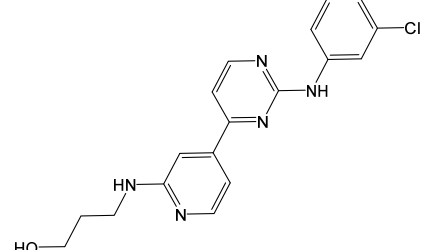
Figure S10. Expression of CAR and CYP2B6 in human hepatocytes, hiPSC-CM, and TNBC cells. Total RNA was isolated from cultured HPH, hiPSC-CM, and TNBC cells. Relative mRNA expression of genes encoding for CAR (A) and CYP2B6 (B) was evaluated in HPH from 3 liver donors (HL#159, HL#166, HL#168), five TNBC cell lines (BT549, HCC38, MDA-MB-231, MDA-MB-468, HCC70), and hiPSC-CMs, respectively. Expression values are presented as fold changes normalized to the level of hiPSC-CMs, which was designated as 1. Results are expressed as mean \pm SD (n=3). ND: Nondetectable.

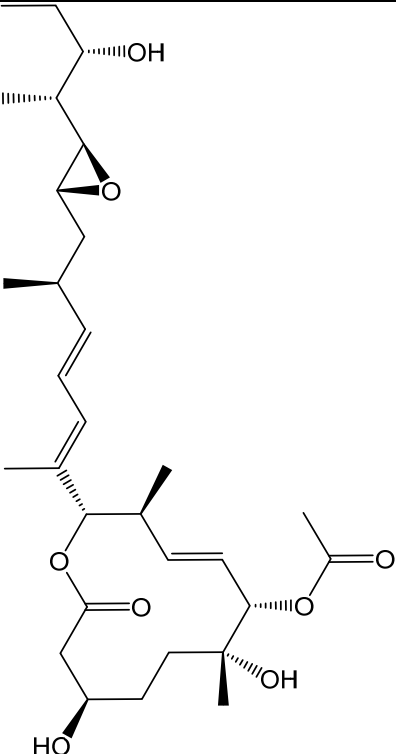
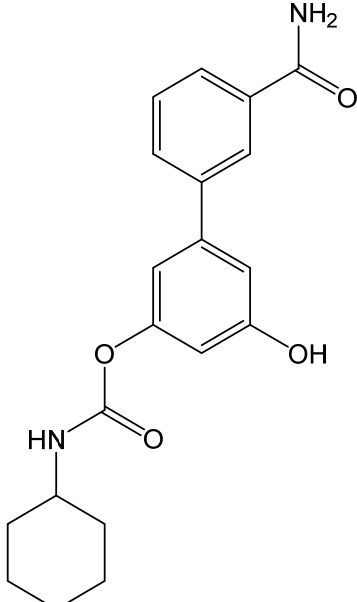
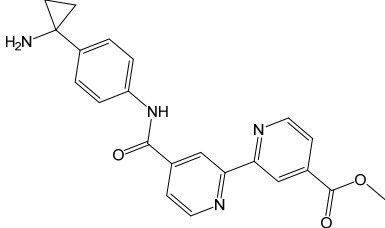
Table S1| Dual activators of hCAR and Nrf2 identified from HTS assays

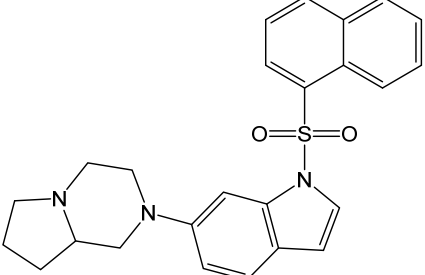
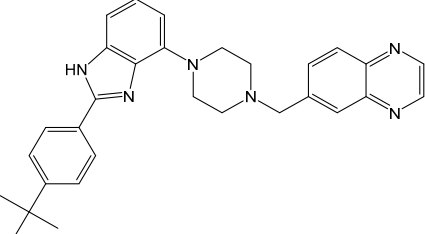
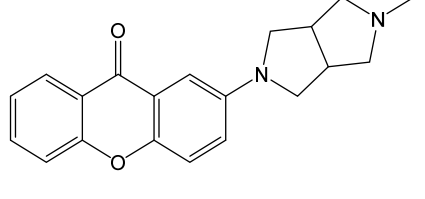
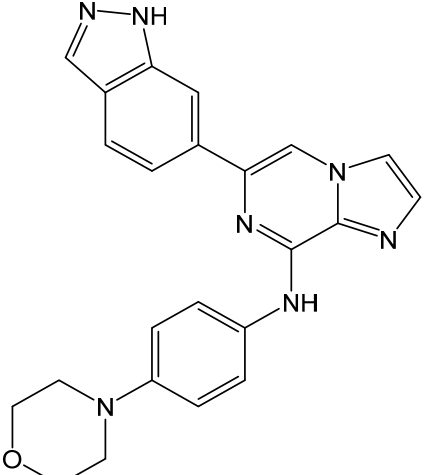
Compound	Structure	EC ₅₀ CAR (μ M)	Efficacy CAR (% Positive Control)	EC ₅₀ Nrf2 (μ M)	Efficacy Nrf2 (% Positive Control)
Necrostatin-1 CN01		5.42 \pm 2.5	12.2 \pm 2.88	2.00 \pm 0.341	62.5 \pm 7.28
NS 9283 CN02		4.82 \pm 1.80	151 \pm 7.85	2.02 \pm 0.504	60.7 \pm 9.01
STF-62247 CN03		7.43 \pm 2.65	152 \pm 15.1	7.86 \pm 2.72	107 \pm 14.5
MMPIP hydrochloride CN04		1.34 \pm 0.307	94.7 \pm 8.12	1.14 \pm 0.275	19.1 \pm 15.1
Dehydrocostus Lactone CN05		1.87 \pm 0.215	51.6 \pm 4.14	3.03 \pm 1.17	94.6 \pm 17.3
DL7076 CN06		8.85 \pm 0.188	140.0 \pm 15.0	0.718 \pm 0.034	73.9 \pm 4.76
Linsitinib CN07		2.35 \pm 0.00	65.2 \pm 4.41	1.88 \pm 0.00	101 \pm 4.20
ML115 CN08		4.56 \pm 2.33	73.7 \pm 9.53	4.27 \pm 0.797	56.5 \pm 7.40

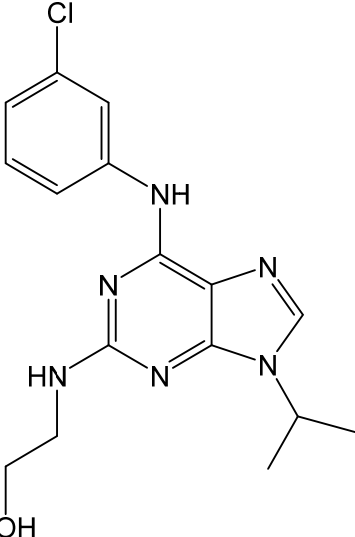
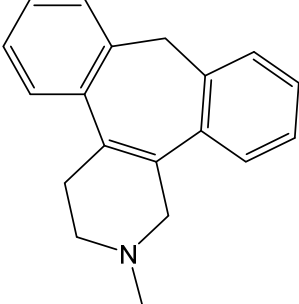
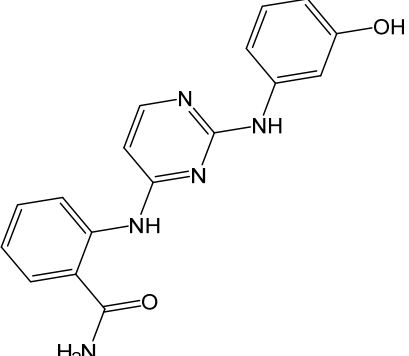
Erlotinib CN09		2.01 ± 0.845	88.3 ± 14.5	3.94 ± 0.709	69.8 ± 5.72
Methyl (2Z,3E,5E,7E,9E)- 2-ethylidene-11-[4- hydroxy-4-(2- hydroxyethyl)-2-oxo-6-oxa- 3-azabicyclo[3.1.0]hexan-1- yl]-4,10-dimethyl-11- oxoundeca-3,5,7,9- tetraenoate CN10		7.83 ± 0.510	109 ± 12.3	5.48 ± 0.446	132 ± 7.51
ML241 CN11		8.37 ± 0.962	90.9 ± 3.84	3.49 ± 2.90	82.8 ± 71.0
4-[(3-Bromophenyl)amino]- 6-acrylamidoquinazoline CN12		3.212 ± 0.442	107 ± 11.7	4.38 ± 0.297	68.6 ± 6.95
Tanshinone I CN13		0.990 ± 0.223	107 ± 11.1	5.99 ± 0.971	77.6 ± 6.16
BLT-4 CN14		6.41 ± 0.882	165 ± 13.2	6.98 ± 0.89	100 ± 5.40
Q94 hydrochloride CN15		6.95 ± 1.25	74.1 ± 8.93	4.76 ± 2.07	54.0 ± 7.03
VU 03610172 hydrochloride CN16		2.56 ± 1.01	97.4 ± 25.9	2.04 ± 0.281	90.5 ± 10.7
XL019 CN17		5.24 ± 3.12	60.9 ± 21.1	4.36 ± 2.08	69.8 ± 9.90

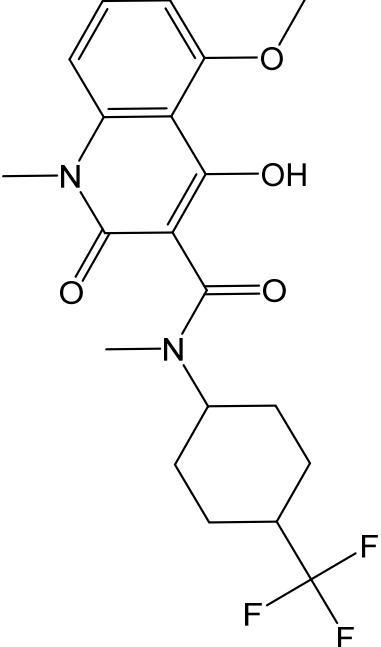
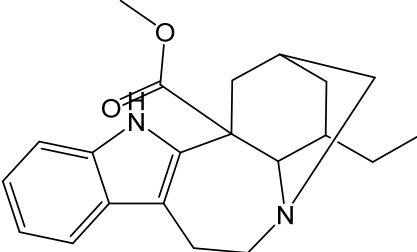
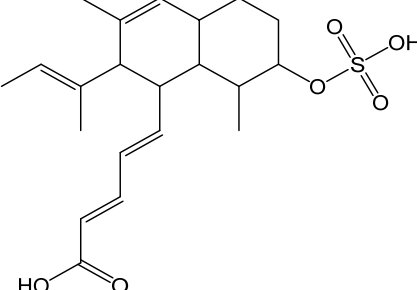
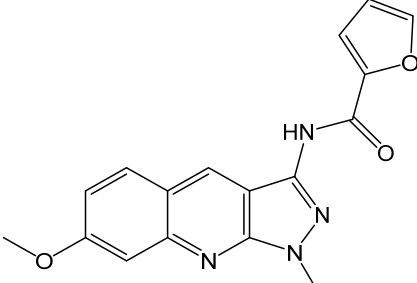
UNC3230 CN18		8.48 ± 1.94	88.4 ± 4.00	1.00 ± 0.081	94.7 ± 5.07
DL7091 CN19		8.48 ± 1.94	88.4 ± 4.00	1.00 ± 0.081	94.7 ± 5.07
DL7092 CN20		10.2 ± 0.122	109.1 ± 48.5	0.054 ± 0.113	41. ± 13.8
Piperine CN21		9.09 ± 1.55	121 ± 8.62	3.69 ± 1.46	49.3 ± 9.43
Gedunin CN22		8.12 ± 0.00	38.7 ± 2.81	2.92 ± 0.336	127 ± 6.84
Pranazepide CN23		4.31 ± 1.39	55.2 ± 1.00	7.54 ± 1.22	45.6 ± 3.26

<p>Motesinib CN24</p>		<p>4.75 ± 0.887</p>	<p>77.1 ± 6.19</p>	<p>6.11 ± 1.95</p>	<p>44.9 ± 4.10</p>
<p>CGI-1746 CN25</p>		<p>9.20 ± 1.06</p>	<p>89.8 ± 17.7</p>	<p>4.77 ± 1.33</p>	<p>36.1 ± 2.57</p>
<p>BTZ043 Racemate CN26</p>		<p>1.44 ± 0.245</p>	<p>82.9 ± 8.36</p>	<p>4.73 ± 0.00</p>	<p>33.0 ± 0.399</p>
<p>CGP60474 CN27</p>		<p>2.96 ± 0.00</p>	<p>74.8 ± 12.7</p>	<p>4.24 ± 0.687</p>	<p>56.7 ± 6.31</p>

<p>Pladienolide B CN28</p>		<p>0.0120 ± 0.00300</p>	<p>98.4 ± 12.4</p>	<p>0.00324 ± 0.000446</p>	<p>125 ± 19.5</p>
<p>3'- (Cyclohexylcarbamoyloxy)- 5'-hydroxy-1,1'-biphenyl-3- carboxamide CN29</p>		<p>8.12 ± 0.00</p>	<p>33.6 ± 1.36</p>	<p>3.28 ± 0.532</p>	<p>40.6 ± 2.44</p>
<p>Methyl 2-[4-[[4-(1- aminocyclopropyl) phenyl]carbamoyl] pyridin-2-yl]pyridine- 4-carboxylate CN30</p>		<p>1.18 ± 0.389</p>	<p>30.5 ± 1.69</p>	<p>6.71 ± 0.771</p>	<p>48.7 ± 5.23</p>

1-(1-Naphthylsulfonyl)-6-(octahydropyrrolo[1,2-a]pyrazine-2-yl)-1H-indole CN31		9.77 ± 1.25	119 ± 9.23	0.375 ± 0.00	34.2 ± 0.00
6-[[4-[2-(4-Tert-butylphenyl)-1H-benzimidazol-4-yl]piperazin-1-yl]methyl]quinoxaline CN32		3.78 ± 1.46	185 ± 66.3	6.80 ± 1.55	31.2 ± 9.13
2-(2-Methyl-1,3,3a,4,6,6a-hexahydropyrrolo[3,4-c]pyrrol-5-yl)xanthen-9-one CN33		4.75 ± 0.322	50.6 ± 1.54	1.28 ± 0.358	44.1 ± 4.42
Entospletinib CN34		0.419 ± 0.048	124 ± 2.98	9.73 ± 10.0	39.1 ± 9.09

NG 52 CN35	 <chem>CC(C)N1C=NC2=C(N1)N=CN2NC3=CC=C(Cl)C=C3NCCC(O)</chem>	2.02 ± 0.131	34.8 ± 6.77	4.73 ± 0.00	49.4 ± 2.78
Setiptiline CN36	 <chem>C1CCN(C1)c2c3ccccc3n2c4ccccc4</chem>	8.61 ± 2.77	35.2 ± 11.5	1.66 ± 1.01	84.5 ± 19.9
DB07268 CN37	 <chem>NC(=O)c1ccc(Nc2nc3c(ncn3N)Nc4ccc(O)cc4)cc1</chem>	6.65 ± 0.764	40.3 ± 6.87	7.49 ± 0.00	66.9 ± 13.6

<p>Tasquinimod CN38</p>		<p>2.68 ± 0.613</p>	<p>38.8 ± 5.92</p>	<p>2.38 ± 0.274</p>	<p>66.4 ± 16.3</p>
<p>Coronaridine CN39</p>		<p>0.281 ± 0.0390</p>	<p>120 ± 6.18</p>	<p>8.24 ± 0.00</p>	<p>38.8 ± 5.72</p>
<p>(2E,4E)-5-[2-[(E)-But-2-en-2-yl]-3,8-dimethyl-7-sulfoxy-1,2,4a,5,6,7,8,8a-octahydronaphthalen-1-yl]penta-2,4-dienoic acid CN40</p>		<p>8.82 ± 1.21</p>	<p>30.1 ± 1.14</p>	<p>6.30 ± 0.867</p>	<p>94.6 ± 2.67</p>
<p>ML370 CN41</p>		<p>6.74 ± 1.54</p>	<p>108 ± 11.2</p>	<p>1.68 ± 0.613</p>	<p>61.3 ± 4.63</p>

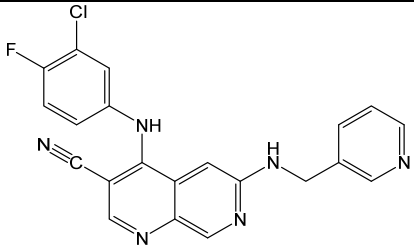
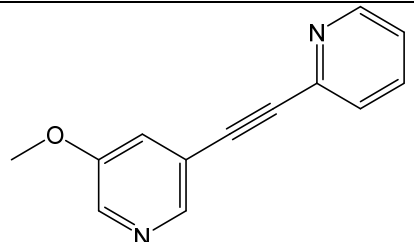
Tpl2 Kinase Inhibitor 1 CN42		2.86 ± 0.394	56.5 ± 7.37	2.90 ± 0.494	65.8 ± 3.13
Methoxy-PEPy CN43		8.44 ± 1.58	51.2 ± 9.74	0.708 ± 0.0576	66.9 ± 13.2

Table S2| Liver Donor Demographics

Donor	Age (years)	Race	Sex	BMI
HL #154	51	Hispanic	Male	29.1
HL #155	32	Caucasian	Male	25.5
HL #156	52	African American	Female	29.9
HL #157	53	Caucasian	Male	33.7
HL #159	64	Caucasian	Male	25.7
HL #160	22	Hispanic	Male	28.9
HL #163	58	Caucasian	Female	28.1
HL #164	56	Caucasian	Male	26.3
HL #166	50	Caucasian	Female	27.3
HL #167	31	Caucasian	Male	24.0
HL #168	65	Caucasian	Male	28.4
HL #171	52	Caucasian	Male	19.7
HL #188	47	Caucasian	Female	23.4

Table S3 Immunostaining and immunoblotting antibodies used

Antibody	Supplier	Catalog Number	IF dilution	WB dilution
CYP2B6	Abcam	Ab140609	-	1:500
CYP3A4	Millipore Sigma	AB1254	-	1:5000
HO-1	Abcam	Ab13248	-	1:1000
Cleaved-Caspase 3	Cell Signaling	#9661	1:100	1:1000
Nrf2	Abcam	Ab137550	-	1:1000
TATA-Binding Protein	Santa Cruz	SC-273	-	1:500
β -actin	Millipore Sigma	MABT825	-	1:3000
horseradish peroxidase goat anti-mouse	Cell Signaling	#7076	-	1:2000
Horseradish peroxidase anti-rabbit	Cell Signaling	#7074	-	1:2000
mouse-anti-phospho-H2AX	Millipore	SER139, clone JBW301	1:500	-
OCT4	Cell Signaling	#2750	1:100	-
TRA-1-60	Millipore	MAB4360	1:200	-
α -actinin	Abcam	ab68167	1:200	-

Supplementary Methods:**Spheroid Culture & Cell Death Assessment**

BT549 and H9c2 cells were seeded in ultra-low attachment 96 well plates (7007, Corning) at 2.5×10^4 and 4×10^4 , respectively. After centrifugation for 2 min at 200 RPM, cells were cultured in incubators at 37 °C, 5% CO₂ for 48-72 h to allow spheroid formation. Subsequently, spheroids were pre-treated with vehicle control (0.1% DMSO) or CN06 (10 μM) for 2 h and cotreated with DOX (2.5 μM) for another 24 h. Cell viability in the spheroids was measured using the NucBlue Live ReadyProbe (R37605, Thermofisher) and NucRed Dead 647 ReadyProbe (R37113, Thermofisher) Reagents following the manufacturer's instructions. Celigo Image Cytometer (Nexcelom) was used to evaluate the integrated intensity ratio of dead over live spheroids normalized to the vehicle control group by scanning for fluorescence at RT.

Spheroid Confocal Microscopy Analysis

In separate experiment, treated spheroids were washed 3X with PBS for 5 min each and transferred from 96 well to Eppendorf tubes (20 spheroids/tube/group). Spheroids were fixed with 4% paraformaldehyde overnight at 4 °C. Fixed spheroids were embedded in Tissue-Tek OCT, sectioned at 8 microns, and mounted on polylysine coated slides. Spheroids were blocked with 10% fetal bovine serum (FBS) for 30 mins. Subsequently, slides were incubated with primary antibodies [phosphor-H2AX (1:100) or cleaved caspase 3 (1:100)] diluted in blocking solution at 4 °C overnight. Secondary antibodies, AlexaFluor 488 (anti-rabbit, 1:200, Fisher Scientific) and AlexaFluor 594 (anti-mouse, 1:200, Fisher Scientific), were diluted in the blocking solution and incubated for 1 h in the dark at RT. Fluoroshield mounting medium with

DAPI (ab104139, Abcam) was added. The fluorescence was viewed using confocal microscopy (Nikon) with a FITC and Texas Red filter at $10\times$ magnification.

Immunocytochemistry for hiPSC-CMs

Differentiated hiPSC-CMs were seeded at 5×10^4 per 35mm dish. Three days after seeding hiPSC-CMs were treated with CN06 or vehicle control for 24 h followed by DOX (1 μ M) cotreatment for another 24 h. Mitotracker (Thermofisher) was added 30 mins prior to fixation. Subsequently, hiPSC-CMs were fixed with 4% paraformaldehyde for 15 mins at RT followed by permeabilization with 1% Triton X-100 for 20 mins. Specimens were blocked with Superblock (37515, Thermofisher) for 1 h at RT. Slides were stained with cardiac Troponin T (ab45923, 1:200) and cardiac α -actinin (ab68167, 1:1000) antibodies diluted in blocking solution overnight at 4°C. Secondary antibody stains were performed by using fluorophore-conjugated secondary antibodies (AlexaFluor 488 and 568) for 1 h in the dark at RT. Prolong Gold Antifade with DAPI (Thermofisher) was used to mount after washing $3\times$ with PBS. Slides were visualized using a Nikon A1 point-scanning laser confocal microscope. Magnification is shown at $60\times$. Quantification was achieved by determining 10 normal sarcomere structures vs sarcomeric disarray per condition. Normal sarcomere structure was observed as extensive bundles of myosin-containing filaments, while sarcomeric disarray was defined as attenuated and disrupted sarcomeres.